SIEMENS

White Paper

Iterative Metal Artifact Reduction (iMAR): Technical Principles and Clinical Results in Radiation Therapy

Marc Kachelrieß, German Cancer Research Center (DKFZ), Heidelberg, Germany
Andreas Krauss, Siemens Healthcare

Introduction

Computed Tomography is a highly accurate and quantitative diagnostic imaging modality that allows to obtain precise information about the patient's density distribution within a few seconds of scanning at sub millimeter spatial resolution.

Nevertheless, there are sources of artifacts that make the images less quantitative than desired. A very prominent artifact is caused by the presence of high density objects in the field of measurement. In most cases such very dense objects are comprised of metal, such as dental fillings, screws and fixations, or as hip or knee implants. Therefore the artifacts are known as metal artifacts, although other sources, such as highly concentrated iodinated contrast agents, may cause similar type of image degradation.

Metal artifacts are generated by four physical effects: beam hardening, scatter, undersampling, and photon starvation.

Beam hardening changes the spectrum of the beam such that the total attenuation is underestimated and the resulting images will show dark streaks or bands along such directions where the x-rays are most strongly attenuated. Scatter artifacts have a very similar appearance. They are caused by scattered photons that make a detour around the metal object and are registered by a detector just behind the metal. Undersampling artifacts occur as white thin streaks emerging from the implant. They are caused by large density differences between the metal and the surrounding tissue which would require much higher sampling to be imaged adequately.

Photon starvation means that only few photons make it through the dense objects. The few photons that are detected are statistically highly uncertain. Therefore white and dark thin noise streaks may result from the presence of metal objects.

Several approaches to reduce or remove the metal artifacts are known from the literature. In mild situations one may choose more adequate scan parameters, or one may algorithmically invert the physical effect (by, for example, performing a beam hardening correction[1]).

In many metal artifact cases, however, there is no usable information in the detector readings behind the metal and these metal shadows need to be replaced by some surrogate data, e.g. by inpainting the data gaps using linear interpolation[2]

Unfortunately, almost all inpainting approaches tend to introduce new artifacts making the results neither valuable for diagnostics, nor for radiation therapy planning.

Just recently, a promising inpainting method[3,4] operating on a normalized sinogram instead of the original raw-data has been proposed and was shown to provide clinical valuable results.

In addition, a so-called frequency split technique[5,6] turned out to successfully restore the original noise texture and restore high frequency details that may have been lost during inpainting.

[1]R. Raupach, H. Shukla, C. Amies, W. Loeffler, MARIS – Metal Artifact Reduction in Image Space – Technical Principles, Siemens Healthcare, 2013

[2]Kalender, Willi A. and Hebel, Robert and Ebersberger, Johannes, Reduction of CT Artifacts Caused by Metallic Implants. Radiology 164(2) 576 – 577, August 1987.

[3]E. Meyer, R. Raupach, M. Lell, B. Schmidt, and M. Kachelrieß. Normalized metal artifact reduction (NMAR) in computed tomography. Med. Phys. 37(10):5482-5493, October 2010.

[4]M. Lell, E. Meyer, M. Küfner, M. May, R. Raupach, M. Uder, and M. Kachelrieß. Normalized metal artifact reduction in head and neck computed tomography. Investigative Radiology 47(7):415-421, July 2012.

[5]E. Meyer, R. Raupach, M. Lell, B. Schmidt, and M. Kachelrieß. Frequency split metal artifact reduction (FSMAR) in CT. Med. Phys. 39(4):1904-1916, April 2012.

[6]M. Lell, E. Meyer, M. Schmid, R. Raupach, S. May, M. Uder, and M. Kachelrieß. Frequency split metal artefact reduction in pelvic computed tomography. European Radiology 23:2137-2145, March 2013.

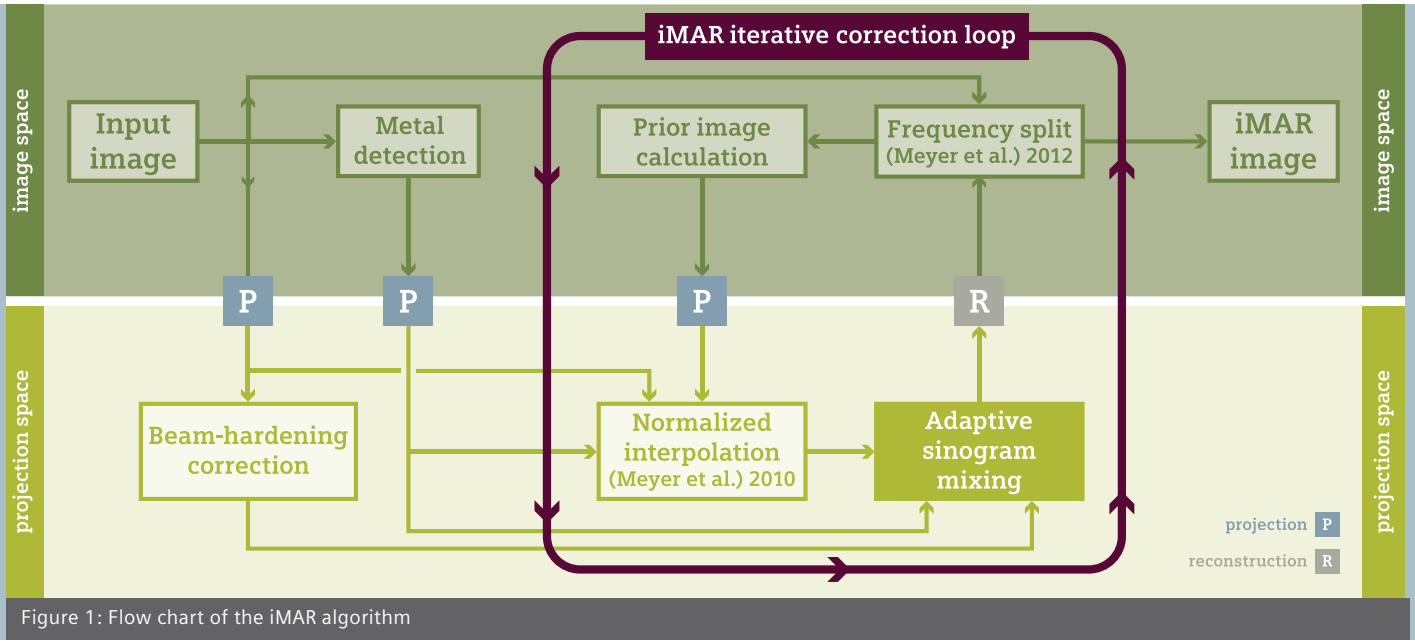

Figure 1: Flow chart of the iMAR algorithm

The iMAR Algorithm

The iMAR metal artifact reduction algorithm combines all three successful approaches: beam hardening correction (in sinogram regions of less severe metal attenuation), normalized sinogram inpainting (in sinogram regions of high metal attenuation), and frequency split (to mix back noise texture and sharp details that are potentially lost during inpainting). The correction process is then iteratively refined by repeating the normalized sinogram inpainting and the mixing steps up to six times. The processing steps are detailed in the following paragraphs, and they are illustrated in the flow chart of figure 1.

Metal detection

Metal artifacts are caused by very dense objects or regions. These can be reliably detected using a thresholding process in the original, uncorrected CT images. The thus-detected extremely dense regions are converted to sinograms by forward projection. Those metal sinograms are zero in regions not influenced by the metal artifacts, and they are non-zero in regions where a combination of beam hardening correction and normalized inpainting shall occur.

Beam hardening correction

The sinogram of the original, uncorrected image is beam hardening corrected in those regions that are influenced by metal (non-zero regions of the metal sinogram). The metal beam hardening correction is based on a two-dimensional projection data correction model. A correction value for each element of the input data is obtained as a function of the total signal attenuation and the portion of the attenuation induced by the metal.

Prior sinogram

A prior image is calculated from the CT image by assigning the CT value of water (0 HU) to metal and soft tissue pixels, while bone, air and lung tissue pixels remain unchanged. Classification into metal, bone, soft tissue, and lung tissue is performed through a Hounsfield number thresholding process. The prior image is forward-projected to obtain the prior sinogram.

Normalized Interpolation

The initial sinogram is divided pixel wise by the prior sinogram. Inpainting is performed on this normalized sinogram. This is done by one-dimensional linear interpolation in channel direction within the metal trace. Then, the normalized sinogram is denormalized by pixel wise multiplication with the prior sinogram.

Adaptive sinogram mixing

The inpainted sinogram is mixed with the beam hardening corrected sinogram according to the total metal attenuation. Sinogram pixels corresponding to low metal attenuation are preferably taken from the beam hardening-corrected sinogram while those corresponding to larger metal attenuation are preferably taken from the inpainted sinogram.

The user interface of iMAR is fairly simple. Besides the typical reconstruction parameters, it only requires to select the desired protocol from a drop down menu. For example, if metal artifacts due to dental fillings are expected, the iMAR protocol “Dental Fillings” is to be selected.

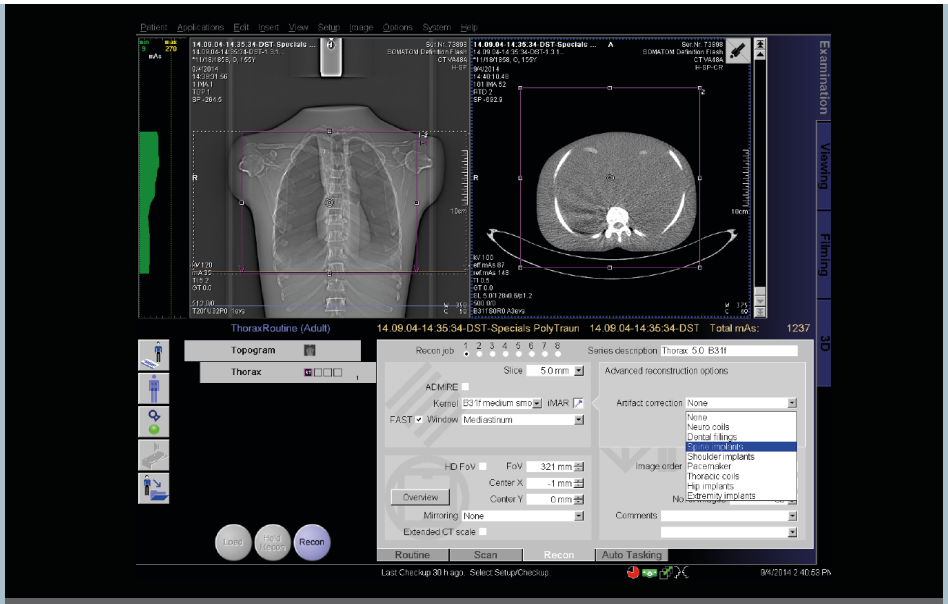

Figure 2: User interface of iMAR

Frequency split

The adaptively mixed sinogram is reconstructed. Then, it is low-pass filtered and the original, uncorrected image is high pass filtered, with the low and high pass filters being complementary. Both filtered images are added to obtain the metal artifact-corrected image. A potential drawback of the frequency-split operation is the reinsertion of high-frequency streak artifacts into the corrected images.

The thus-corrected image is now taken as a starting point for the next iterations. It is used to generate a new prior sinogram. With this another inpainting, adaptive sinogram mixing and frequency split is performed. Up to six such iteration steps are performed before the final iMAR-corrected image is obtained. Figure 2 gives an impression of iMAR’s user interface.

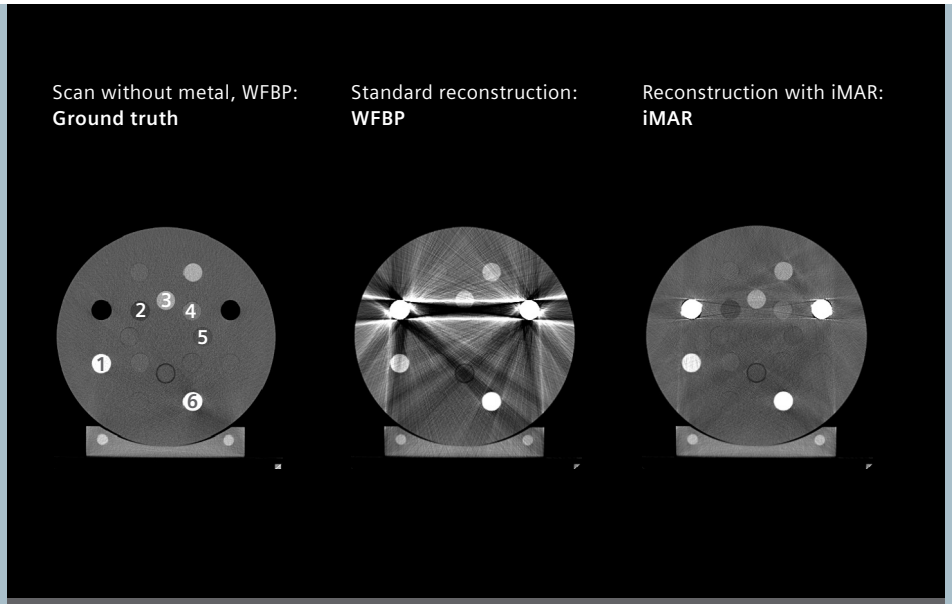

Figure 3

Gammex phantom (33 cm) without and with metal inserts (28 mm). The ground truth is the measurement without metal inserts (left). The standard reconstruction of the data with metal inserts (center) shows significant metal artifacts. The iMAR-reconstructed image (right) is of low artifact content. The noise texture is well preserved, even in the region between the metal inserts. C = 0 HU, W = 800 HU.

Phantom Examples

To quantify the performance of the iMAR algorithm phantom scans were carried out. The phantoms were equipped with and without metal inserts. Scans without the metal inserts serve as the ground truth, while those with metal objects serve to demonstrate the geometrical and gray value accuracy without and with the application of iMAR. In addition, treatment plans were computed from the scans. To obtain a comparable treatment plan for the ground truth images, i.e. those that were scanned without metal objects, the metal was manually inserted into these images. This was done using the planning system as follows: The metal was segmented in the WFBP images and added to the metal-free images.

Figures 3 and 4 give an example of iMAR's performance under the presence of two steel objects inserted into the widely used Gammex phantom. While the WFBP reconstruction shows significant metal artifacts, the iMAR images are almost artifact-free. To become more quantitative we assessed the CT-values of six representative Gammex inserts. The results are shown in in table 1. They confirm what we already found from the difference images of figure 4: iMAR achieves to restore the true CT-values to a high degree of accuracy.

With WFBP, i.e. without iMAR, the deviations of the Gammex CT values from the ground truth are mostly larger than 100 HU in our experiment. In some cases they even exceed 400 HU. The iMAR reconstruction consistently reduces those errors to the order of about 20 HU which lies in the range of the image noise level.

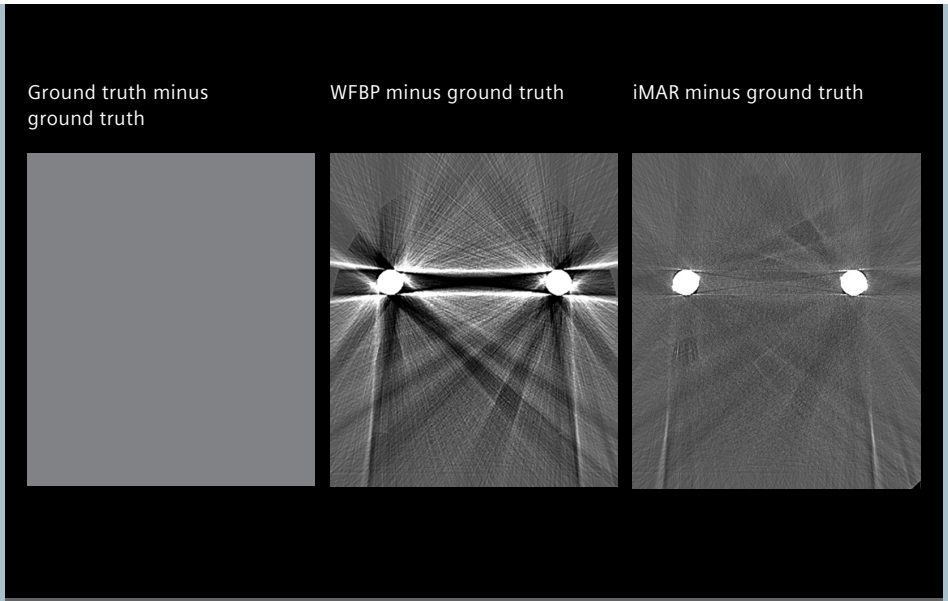

Figure 4

The difference of the WFBP and the ground truth (center) reveals that the metal artifacts significantly change the CT values. Obviously, iMAR restores the true Hounsfield values with a very high degree of accuracy (right). C = 0 HU, W = 800 HU.

Insert #	Description	Ground Truth (GT)	Weighted Filtered Back Projection (WFBP)	attenuation deviation |(GT – WFBP) ÷ (1000 + GT)|	iMAR	attenuation deviation |(GT – iMAR) ÷ (1000 + GT)|
1	CB2-30%	414 HU	266 HU	10%	391 HU	2%
2	Adipose	-90 HU	-507 HU	46%	-59 HU	3%
3	Inner Bone	197 HU	376 HU	15%	201 HU	0.30%
4	Liver	64 HU	-366 HU	40%	78 HU	1%
5	Breast	-41 HU	-136 HU	10%	-35 HU	0.60%
6	CB2-50%	675 HU	575 HU	6%	671 HU	0.20%

Table 1: Quantitative evaluation of the CT values obtained in the Gammex phantom.

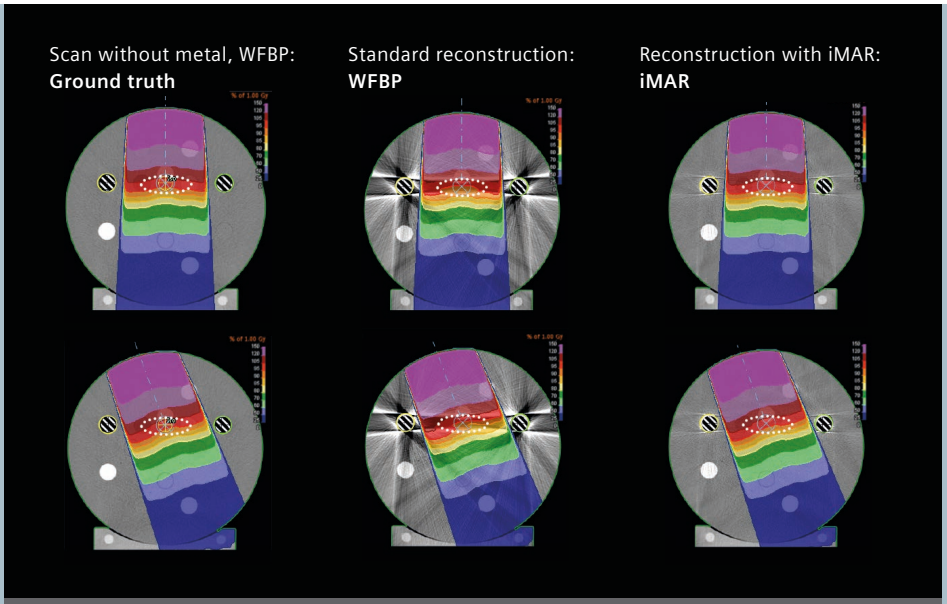

Figure 5

Dose distribution for a single static 6 MV treatment beam entering the phantom from 0° (top) and from -20° (bottom). The contours are colored in 5% and 10% steps relative to the dose of the reference area (dotted ellipsoids). Identical iron inserts (shaded circles) were assumed for all three dose calculations. Ideally, the dose distribution should match the dose distribution of the ground truth. This, however, is not the case for the WFBP image (center) because the metal artifacts cause dose distribution distortions due to the presence of artifact. With iMAR (right) the calculated dose distribution is nearly identical to the ground truth. C = 0 HU, W = 800 HU

The strong metal artifacts impair the accuracy of the Hounsfield values. Thus it is to be expected to observe an influence of the calculated dose values, too. To demonstrate this influence we calculated the dose distribution of a single 6 MV static treatment field entering (field size 8 cm × 5 cm) the Gammex phantom from above (0° gantry angle) and for a slightly tilted field (-20° gantry angle). The dose distributions were computed using a collapsed cone algorithm. The results are shown in figure 5.

In case of the WFBP reconstruction significant distortions of the calculated dose distributions can be seen. In contrast thereto, the dose distribution calculated from the iMAR images is very similar to the dose distribution calculated from the ground truth images.

Focusing on a hypothetical planning target volume (PTV) that significantly overlaps with the metal artifacts (dotted ellipsoids in figure 5) we find that the dose to the PTV is about 5% off the true dose in the WFBP case, while iMAR predicted the correct dose level. Hence a treatment based on the WFBP image would exceed the desired dose level to the PTV by about 5%. Considering that a typical target dose easily exceeds 20 Gy an error of 5% corresponds to an absolute error of 1 Gy or more.

External fixations are a particular challenge for inpainting-based MAR algorithms because the area to be inpainted connects soft tissue background with air background. From left to right (first row): image without metal screw, uncorrected image, reconstruction with standard WFBP (with metal screw), reconstruction with iMAR and intended wrong profile (with metal screw), reconstruction with iMAR and the correct profile (with metal screw). Bottom row: top row minus ground truth. C = 0 HU, W = 800 HU.

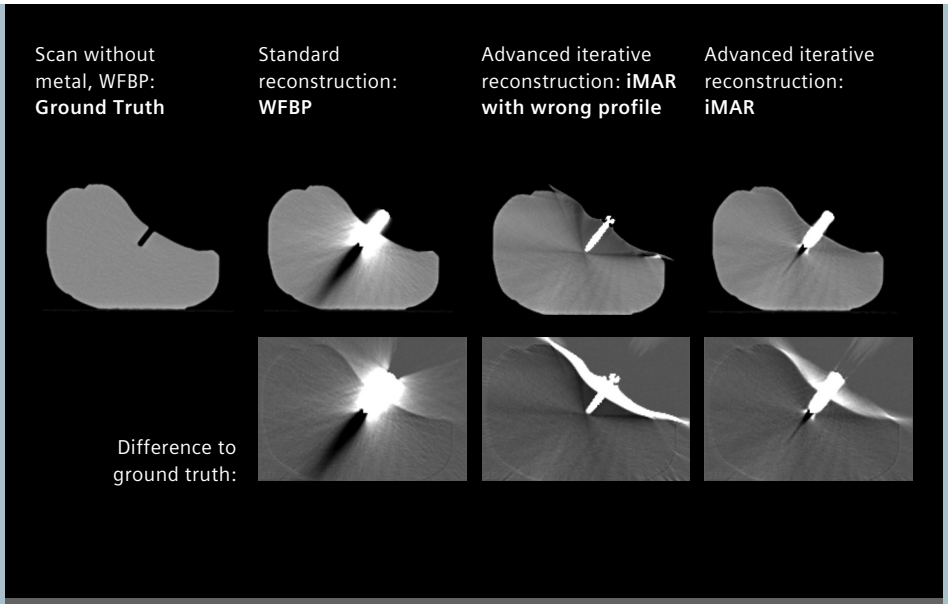

Figure 6

Although iMAR appears to behave well in most reasonable cases we constructed a case where a metal screw is partially exterior to the patient. We thereby intend to provoke a failure of iMAR. The reasoning behind this setup is that the inpainting process will encounter projections where the metal shadow is not fully contained in soft tissue or bone but where it is rather surrounded in parts by air. Figure 6 presents the images of a foot phantom with a surgical screw extending into air. The WFBP image shows the typical metal artifacts.

If the wrong iMAR profile is chosen, iMAR may close the soft tissue region by its convex hull (third column).

Such a behavior is also known from metal artifact reduction algorithms available on the market. With the correct iMAR profile “extremity implants”, the iMAR images appear to represent the correct surrounding anatomy (right column).

A closer look, however, reveals that the CT values in the air region close to the metal are far too high with iMAR. This can best be seen regarding the difference images in the second row of figure 6. Thus the case of external fixations and screws is a limitation of iMAR and care has to be taken in similar cases.

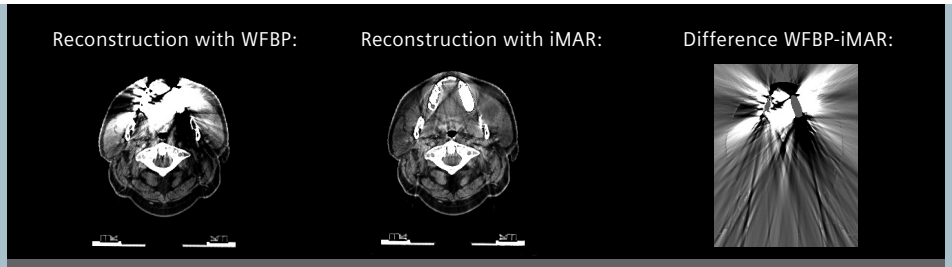

Figure 7: Head patient with significant metal artifacts due to dental fillings. C = 40 HU, W = 350 HU.

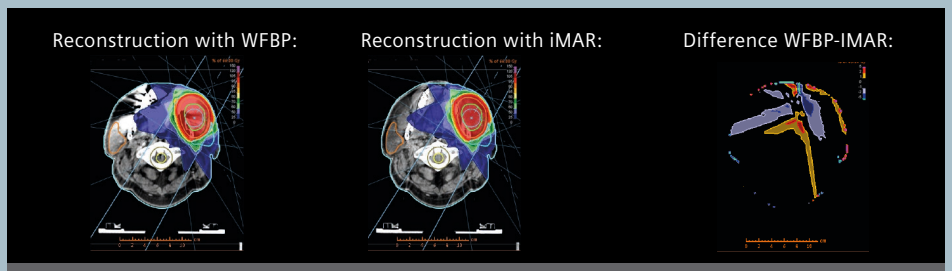

Figure 8

Figure 8: Dose distribution for a 40 segment step-and-shoot treatment plan. The differences in dose distribution differences between WFBP (left) and iMAR (center) are seen in the CT images. The difference dose distribution map (right) reveals them quite clearly and quantitatively the relative error may be as high as 4%. C = 40 HU, W = 350 HU.

Patient Data

Figure 7 shows a patient with a metastasis to the musculus masseter (masseter muscle). The dental fillings or implants cause significant metal artifacts that obscure parts of the tumor, the soft tissue between the roots, and most other soft tissue connecting to the teeth. It should be noted that the metal artifacts cause an increase of the CT-values in some regions while in other regions the attenuation values appear to be significantly lowered. With iMAR most parts of the patient can be recovered. The iMAR image is not free of artifacts, but provides a considerable improvement over the WFBP reconstruction.

A step-and-shoot treatment plan was computed for that patient using the RayStation treatment planning software (RaySearch Laboratories AB, Sweden). The plan was based on the WFBP images and comprises six intensity-modulated 6 MeV beams, each beam consisting of around 7 segments, with 40 segments in total. The corresponding dose distributions is shown in figure 8.

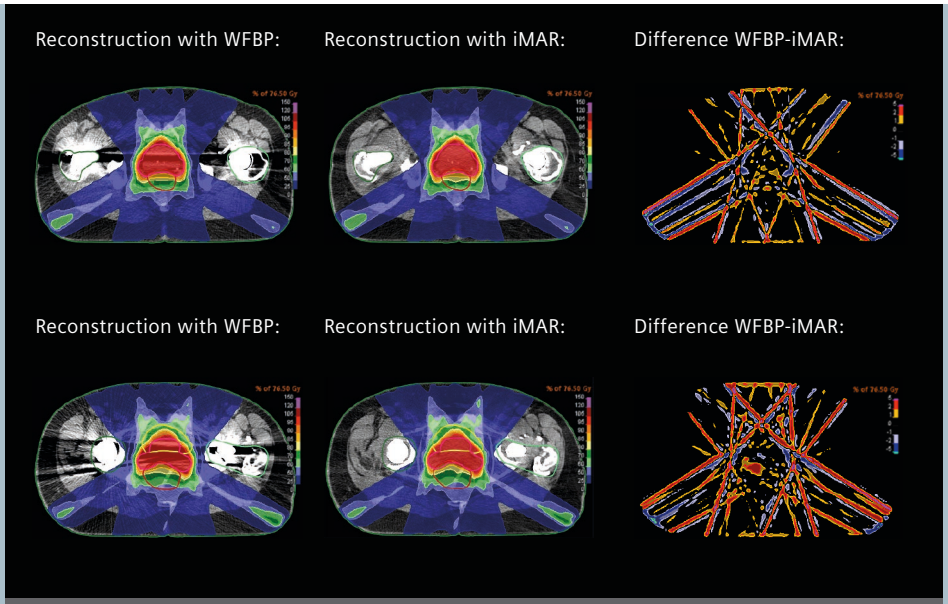

Figure 9

Figure 9: Patient (courtesy of Radiologische Allianz Hamburg, Germany) with a bilateral hip prosthesis. IMRT treatment with 7 beams at 6 MV. The difference map shows the effect of the iMAR algorithm which provides images with more consistent attenuation information and with less artifacts. C = 40 HU, W = 350 HU.

In addition the same treatment plan was used for a dose calculation based on the iMAR images, which may be useful for verification. The differences found between the dose calculation based on WFBP and the one based on iMAR (right image of figure 8) reveal a potential dose misestimation by as much as 4% if the WFBP images are used for the dose calculation.

Similar advantages of iMAR are seen in other body regions. Figure 9, for example, shows images of a patient with hip implants. The strong metal artifacts in the WFBP image are significantly reduced with iMAR and, thereby, more accurate attenuation values are reconstructed. The differences between the dose maps are as large as 5%.

Discussion and Conclusion

The iterative metal artifact reduction (iMAR) software is a valuable tool to significantly improve images obscured by metal artifacts. The benefits of improved image quality are also visible in the improved accuracy of calculated treatment dose distributions and thereby iMAR appears to be a potentially valuable tool to improve the generation of treatment plans. The potential benefits include the improved visibility of tumors on the one hand, and the improved accuracy of the reconstructed attenuation values on the other hand. With iMAR, treatment plans may become more accurate, which includes a better dose distribution, with potentially lower doses to organs of risk and potentially helps optimizing the dose to the planning target volume. Further evaluation is needed to substantiate our results which are based on a small number of patient cases.

* This patient has been scanned at Radiologische Allianz Hamburg

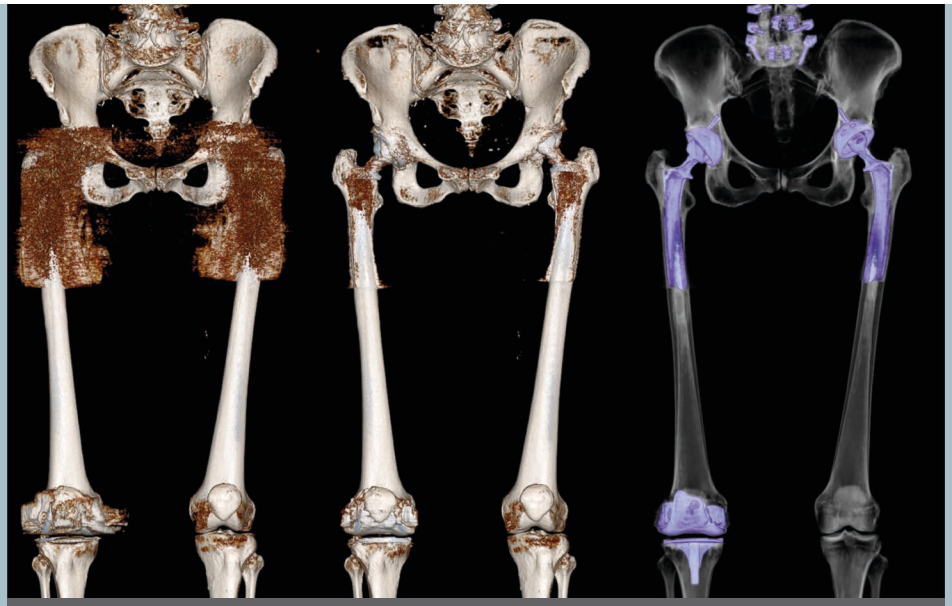

Figure 10

Figure 10: Volume rendered patient case with two hip implants, reconstructed with FBP and iMAR. Third picture on the right changes visualization of bones to semi-transparent, thus metal can be more easily identified.

However, there are also limitations to the use of iMAR: It is always to be kept in mind that iMAR performs inpainting to fill data gaps with reasonable values. In certain ill-posed cases iMAR may fail to reproduce the correct body outline. Therefore it is always recommended to visualize and cross-check both sets of images, the WFBP images and the iMAR images.

It should further be noted that water substitution is sometimes used in those cases where no metal artifact reduction software is available. While "the HU value filling" approach, which consists of manually delineating the soft tissue regions and replacing the regions with the attenuation properties of water, will also reduce the dose estimation errors to some extent, water substitution is quite labor intensive and introduces another delay in the radiation treatment workflow.

Using iMAR, such water substitution techniques can potentially be avoided, thereby supporting an increase in treatment plan accuracy and reducing the time required for treatment planning.

In conclusion, iMAR is a highly promising artifact reduction technique with potential benefits for treatment plan optimization and verification, and may enable time savings when treating patients with metal implants.

Acknowledgements

Esther Bär and Stefan Kuchenbecker, German Cancer Research Center, Heidelberg, Germany, have helped to prepare the data and content of the manuscript.

In the event that upgrades require FDA clearance, Siemens cannot predict whether or when the FDA will issue its clearance. Therefore, if regulatory clearance is obtained and is applicable to this package, it will be made available according to the terms of this offer.

On account of certain regional limitations of sales rights and service availability, we cannot guarantee that all products included in this brochure are available through the Siemens sales organization worldwide. Availability and packaging may vary by country and are subject to change without prior notice. Some/All of the features and products described herein may not be available in the United States.

The information in this document contains general technical descriptions of specifications and options as well as standard and optional features which do not always have to be present in individual cases.

Siemens reserves the right to modify the design, packaging, specifications, and options described herein without prior notice. Please contact your local Siemens sales representative for the most current information.

Note: Any technical data contained in this document may vary within defined tolerances. Original images always lose a certain amount of detail when reproduced.

siemens.com/imaging-for-RT

International Version. Not for distribution in the U.S.

Siemens Healthcare Headquarters
Siemens Healthcare GmbH
Henkestr. 127
91052 Erlangen
Germany
Phone: +49 9131 84-0
siemens.com/healthcare

Order No. A91RO-07052-09C1-7600 | Printed in Germany | CG 2609 0115.06 |

siemens.com/healthcare